Relationship Between Morphology and Rheology of PA/PE/Clay Blend Nanocomposites. I. PA Matrix

S. Malmir,[1,2] M. K. Razavi Aghjeh,[1] M. Hemmati,[2] R. Ahmadi Tehrani[1]

[1]*Institute of Polymeric Materials, Polymer Engineering Department, Sahand University of Technology, Sahand New Town, Tabriz, Iran*
[2]*Department of Polymer Science & Technology, Research Institute of Petroleum Industries, RIPI, Tehran, Iran*

Received 4 April 2011; accepted 3 November 2011
DOI 10.1002/app.36439
Published online 31 January 2012 in Wiley Online Library (wileyonlinelibrary.com).

ABSTRACT: Morphology and linear viscoelastic properties of PA/PE/Clay blend nanocomposites with and without compatibilizer (PE-*g*-MA) with PA as a matrix phase were studied. Using rheological and XRD analyses, it was shown that the clay exhibited higher dispersion in PA/PE blend than that in pure PA. It was attributed to the detachment of intercalated clay layers in PA matrix due to the stress transfer of PE particles and deformation flow field created between PE particles, leading to formation of stronger network. The presence of PE-*g*-MA further enhanced the clay dispersion in the blend. While the results of XRD were not able to accurately assess the morphology, using rheological analysis it was predicted that if the clay is first compounded with dispersed PE phase (PE+PE-*g*-MA), the clay could not leave the PE phase but PA diffuses to the composite droplets of (PE+PE-*g*-MA)/Clay to form phase within phase within phase morphology. SEM and TEM analyses confirmed the reliability of the prediction. It was demonstrated that the rheological studies has a reliable sensitivity to the clay dispersion, its localization, and phase morphology of blend nanocomposites. © 2012 Wiley Periodicals, Inc. J Appl Polym Sci 125: E503–E514, 2012

Key words: blend; nanocomposite; rheology; morphology

INTRODUCTION

During the last two decades, polymer/clay nanocomposites have gained great interest due to their attractive technological applications, superior properties, and improved performance of these materials compared with virgin polymers or conventional micro- and macro-composites.[1–4] Although different general techniques such as solution mixing[5,6] and *in situ* polymerization[7–9] are employed to preparing polymer layered silicate nanocomposites (PLSNs) but the melt intercalation is the most industrially valuable technique because of its low cost, high productivity, and compatibility with conventional polymer processing techniques.[9–11] Many different polymers have been employed in preparing polymer/clay nanocomposites via melt intercalation method such as PA, PE, PP, PVC, etc. The obtained frequently results have shown that while organically modified clay could be intercalated in polar polymers such as PA and PVC, for its intercalation beside nonpolar polymers such as PE and PP, a proper compatibilizer such as PE-*g*-MA or PP-*g*-MA should be used.

Correspondence to: M. K. Razavi Aghjeh (karimrazavi@sut.ac.ir).

Journal of Applied Polymer Science, Vol. 125, E503–E514 (2012)

It has been shown that the state of clay dispersion, play a key role in determining of the processability and final properties of PLSN hybrid materials. Intercalated and exfoliated microstructures are the most common types of polymer/clay nanocomposite's morphology.[12–14] Wide-angle X-ray diffraction and transmission electron microscopy (TEM) are the most used direct techniques in evaluation of microstructure of these materials. The XRD results say little about the morphology except that exfoliation is not complete, even then this technique can lead to false and incomplete interpretations of the nanocomposites.[15,16] Direct observation by TEM is needed to get a better understanding of the state of dispersion. However, the main problem with TEM is that the volume probed is very small and may not be representative of the nanocomposite as a whole. Therefore, bulk properties such as rheological properties should be conducted in addition to using both TEM and XRD analyses.

While for pure polymers such as PA and PE, the most important challenge is to study the effect of different affective parameters on the clay dispersion to find a way to control the final microstructure, for polymer blend nanocomposites (clay filled blends) another challenge is that where the clay is located; in matrix phase, dispersed phase, or at the interface. Beside the dispersion state of the clay (intercalated or exfoliated), localization of the clay either in a single phase, both phases or at the interface of a blend,

can influentially affect the different properties of the polymer blend nanocomposites.

As PA and PE have low permeability to oxygen and water, respectively,[17–20] their blends could provide a meaningful barrier behavior to both water and oxygen. In such a blend, the presence of clay may affect its permeability to oxygen and/or water depending on its localization. Therefore, study on the different aspects of such a blend nanocomposite is of interest.

The main objective of this work was to study rheology and morphology of PA/PE/Clay hybrid nanocomposites. It was tried to predict the dispersion state of the clay and its localization in PA/PE blend via linear viscoelastic measurements. Direct analyses such as XRD, SEM, and TEM were also used to confirm the predicted results. Finally, the effect of feeding order on the partitioning of the clay was studied.

TABLE I
Compositions, Codes, and Feeding Orders of all the Samples

Codes and compositions of the samples			
Sample	Code	Composition	Feeding order
PA6	PA	100	1
LDPE	LD	100	1
PA/PE	PA/LD	80/20	1
PA/PE/PE-*g*-MA	PA/LD/M	80/10/10	1
PA/Cloisite 30B	PA/30B	100/3	1
PA/Cloisite 30B	PA/30B 3.75	100/3.75	1
PE/Cloisite 30B	LD/30B	100/3	1
PE/PE-*g*-MA/ Cloisite 30B	LD/M/30B	90/10/3	1
PA/PE/ Cloisite 30B	PA/LD/30B	80/20/3	1
PA/PE/PE-*g*-MA/ Cloisite 30B	PA/LD/M/30B	80/10/10/3	1
PA/(PE/PE-*g*-MA/ Cloisite 30B)	PA/(LD/M/30B)	80/10/10/3	2

EXPERIMENTAL

Materials

The polyamide 6 used in this study was Akulon F223, obtained from DSM Engineering Plastics, Netherlands. The low-density polyethylene was LF0200 (MFI = 2.0 g/10 min; 190°C, 2.16 Kg) obtained from Bandar Emam Petrochemical Company, Iran. Maleic anhydride grafted polyethylene; Overac 18302N, from Arkema Company was used as a compatibilizer. Sodium montmorillonite clay modified with methyl tallow bis-2-hydroxy ethyl quaternary ammonium (Cloisite 30B) was provided by Southern Clay Products (Gonzales, TX).

Preparation of nanocomposites and reference samples

All the samples were prepared in an internal mixer (Brabender W50EHT) with a rotor speed of 60 rpm at temperature of 230°C. To avoid the effect of moisture, all the materials were dried in a vacuum oven at 80°C for 12 h prior to mixing. All the polymeric components were first dry mixed and fed into the chamber. The clay was added to the melt mixture after 6 min of the process beginning and compounding was continued up to 20 min. Obtained samples were compression-molded into suitable pieces for XRD and rheometry analyses. Molding was carried out at 230°C followed by slow water-cooling under low pressure. The weight ratio of PA to PE phase (PE+PE-*g*-MA) was 80/20, the weight ratio of clay to polymeric phase was 3/100 and the weight ratio of compatibilizer to clay was 10/3 for all the samples unless otherwise specified. To study the effect of feeding order, a sample was prepared via two-step compounding method and the obtained results were compared with the results of the same sample prepared via single step method as discussed above. The compositions together with the corresponding codes are listed in Table I.

FTIR analysis

Infrared absorption spectroscopy (ISS88, Bruker, Germany) was used to evaluate the reaction between NH groups of PA and MA groups of PE-*g*-MA. All the samples were compression molded into thin layer of films at 230°C and about 3.0 MPa pressure. The samples were cooled to room temperature in the mold under pressure and then scanning in the range of 400–4,000 cm^{-1} was applied.

Rheological measurements

Specimens for rheological testing were molded in a hot press at 230°C for 2 min. The molded samples were disc shaped with a diameter of 25 and 2 mm thickness. A Rheometric Mechanical Spectrometer (MCR301: Anton Paar) was used to measure the rheological characteristics of nanocomposites and reference samples using parallel plate geometry. The diameter of both upper and lower plates was 25 mm, and the gap between two parallel plates was 1 mm. The rheological measurements were carried out at a fixed temperature of 230°C under a nitrogen gas flow to avoid premature thermal degradation of the samples. Frequency sweep tests were made over a range of 0.0398–625 rad/s at strain of 1%, to maintain the response of the materials in a linear viscoelastic regime.

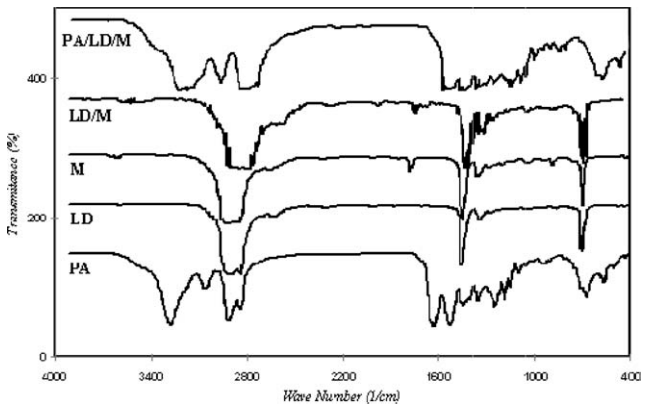

Figure 1 FTIR spectra of neat polymers and their blends.

Morphology characterization

Degree of intercalation/exfoliation of the clay in the nanocomposites and blend nanocomposites was evaluated using X-ray diffractometry (XRD). Thin disks (2 mm) of nanocomposites were prepared by compression molding at 230°C and low pressure for 2 min. X-ray diffraction pattern of the nanocomposites were obtained by using TW3710 Philips X'Pert diffractometer with CuKα radiation. It was scanned over a 2θ range of 1°–10° at the scanning rate of 1.2°/min. The interlayer spacing (d_{001}) of clay was determined from Bragg's equation and the reflection peak in the XRD patterns, for all the nanocomposite and blend nanocomposite samples.

The cryo-fractured surface of the blend nanocomposites and reference blends were inspected in a scanning electron microscope (SEM; XL30, Philips, Holland). The dispersed PE phase was selectively extracted in boiling Xylene for higher contrast. Then the fractured surfaces were coated with a thin layer of gold to avoid electrostatic charging during examination and then micrographs were taken with different magnifications. The transmission electron micrographs were obtained with electron microscope (TEM; CM 200 FEG, Philips, Holland) to examine the dispersion state and partitioning of the clay in blend nanocomposites. Thin sections of about 20–70 nm thickness were cut with a diamond knife in liquid nitrogen.

RESULTS AND DISCUSSION

FTIR analysis

Figure 1 shows the infrared spectra of neat polymers and their blends. Characteristic peaks for PA and PE absorption can be present as follows: at a wave number of 1,640 cm^{-1} C=O stretching vibrations, at 1,560 cm^{-1} N—H bending vibrations, and at 3,300 cm^{-1} N—H stretching vibrations for PA and at 1,472 cm^{-1} C—H stretching vibrations and at around 2,800–2,900 cm^{-1} symmetrical and asymmetrical stretching in $-CH_2$ groups for PE. Characteristic absorption peak of PE-*g*-MA presents at 1,790 cm^{-1} corresponding for anhydride-type carbonyls and 1,710 cm^{-1} for acid-type carbonyls. In the IR spectra of ternary blends (PA/PE/PE-*g*-MA) disappearance of characteristic peak of PE-*g*-MA(1,790 cm^{-1}) is indicative of conversion of anhydride carbonyl groups to $-\overset{O}{\overset{\|}{N-C}}-$ groups in the result of reaction between NH amide or NH_2 amine groups of PA with carbonyl groups of PE-*g*-MA. Occurrence of both type of reactions lead to formation of $-\overset{O}{\overset{\|}{N-C}}-$ group as shown in Scheme 1.[21] In other words, these results show that PA-*g*-PE copolymer is created during the mixing.

Rheological behaviors

The melt rheological properties of nanocomposites provide fundamental insights about the processability and morphology of these materials. Viscoelastic measurements are highly sensitive to the nanoscale and mesoscale structure of the nanocomposites and appear to be a powerful method to probe the state of dispersion in such materials.[22–26] The addition of organoclay to polymer matrix increases the storage modulus by several orders of magnitude and alters the shear thinning behavior at low frequencies to indicate a transition from liquid-like ($G' = \omega^2$, $G'' = \omega^1$) to solid-like (G',$G'' = \omega^0$) rheological behavior.[27] It is generally believed that the extent of these changes reflects the state of dispersion of the clay. This has been attributed to the formation of a percolated network superstructure of the exfoliated layers or stacks of intercalated layers called tactoids.[22,25,26] However, the morphology and interface properties of a blend have strong effect on its rheological properties. Considering the fact that in a nanofiller filled blend system, nanofiller may locate preferentially in a single phase, both phases or at the blend interface, the rheological behavior of the nanocomposite blends becomes more complicated.

Figure 2 presents the results of complex viscosity (η^*) and storage modulus (G') of PA, PE, and their nanocomposites as functions of angular frequency. The results show that both polymers exhibit liquid-like behavior and the PE sample shows higher viscosity and elasticity than PA.

It can be seen that while addition of clay does not clearly affect the rheological properties of PE, it increases the complex viscosity and storage modulus of PA, representative of higher affinity of clay to PA, which in turn can lead to intercalation of clay with PA chains and hindering of the mobility of a large fraction of PA chains because of their contacts with organoclay layers.[21] An appreciable increase in viscosity and elasticity of PA with clay feeding in all frequency ranges, and appearance of a pseudo solid-like

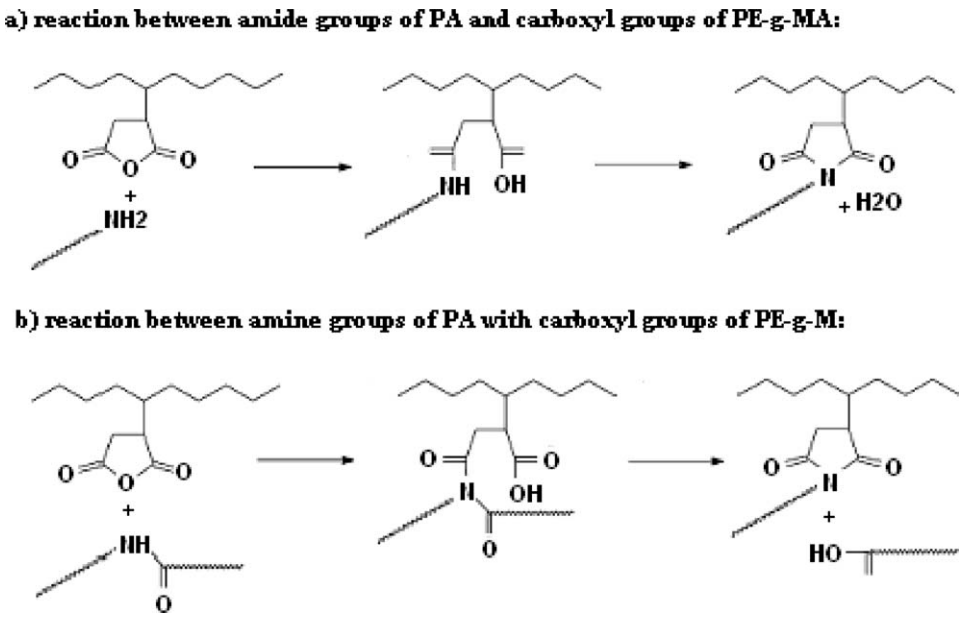

Scheme 1 Schematic of reaction between NH groups in PA and MA groups in PE-*g*-MA.

behavior can be representative of an intercalated and/or exfoliated morphology for this nanocomposite sample. However, a clear plateau of elasticity has not been appeared at low frequencies. This shows that a three dimensional network of the clay has not completely been formed in PA matrix may be due to the lower clay content than that of percolation concentration. The reinforcing effect can also results from the interactions between the components due to hydrogen bonding of hydroxyl groups in the organic surfactant of the organoclay and NH groups of PA chain segments.[28]

The PE/Clay sample exhibits rheological behavior similar to neat PE. This indicates that clay is not exfoliated or intercalated in PE matrix, due to the low interaction between PE and clay. However, the storage modulus of PE/Clay nanocomposite shows a little increase at low frequencies. Although, the presence of PE-*g*-MA has not dramatically changed the rheological behavior of PE/Clay nanocomposite but it has increased both viscosity and elasticity of PE/Clay nanocomposite. Based on this fact that the PE has higher molecular weight than that of PA, in the case, which PE-*g*-MA could facilitate the clay intercalation; the extent of storage modulus increment should be much more than that of PA. These show that PE-*g*-MA increases the interaction between PE and clay tactoids but it cannot influentially increase the layer spacing of the clay.

Figure 3 shows the results of tan δ as a function of angular frequency for different samples. These results clearly show that PE, PE/Clay and PE/PE-*g*-MA/

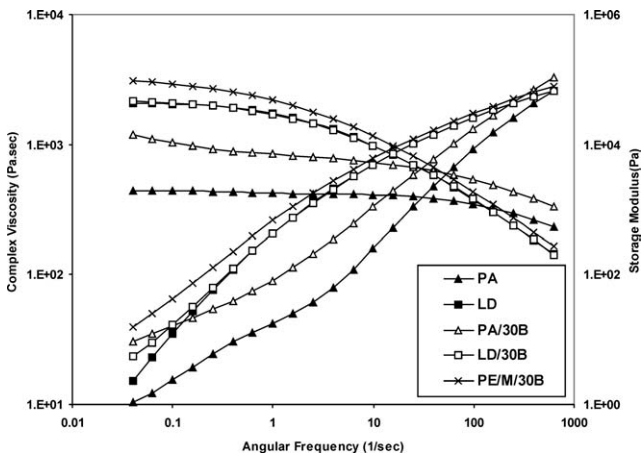

Figure 2 Storage modulus and complex viscosity versus angular frequency of PA, PA/Clay, PE, PE/Clay, and PE/PE-*g*-MA/Clay.

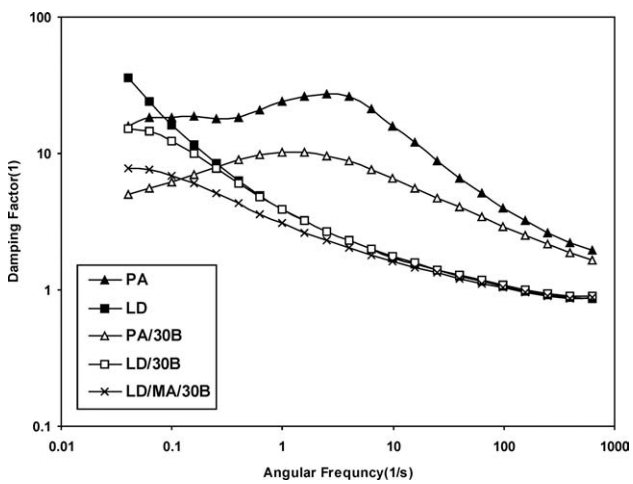

Figure 3 Damping factor versus angular frequency of PA, PA/Clay, PE, PE/Clay, and PE/PE-*g*-MA/Clay.

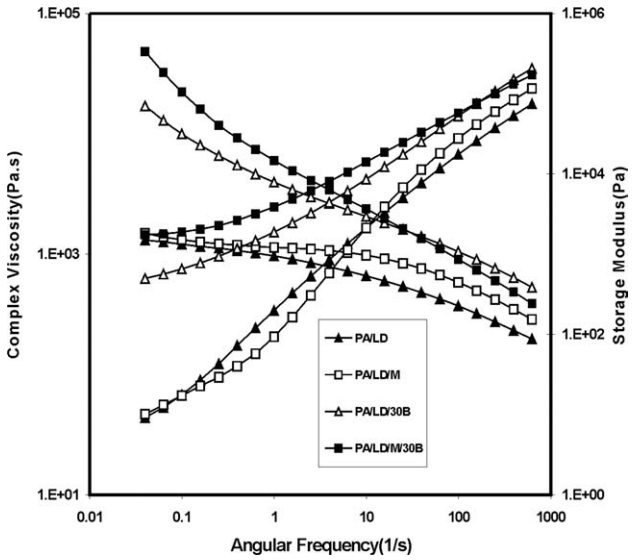

Figure 4 Storage modulus and complex viscosity versus angular frequency of PA/PE/Clay and PA/PE/PE-*g*-MA/Clay and their reference blends.

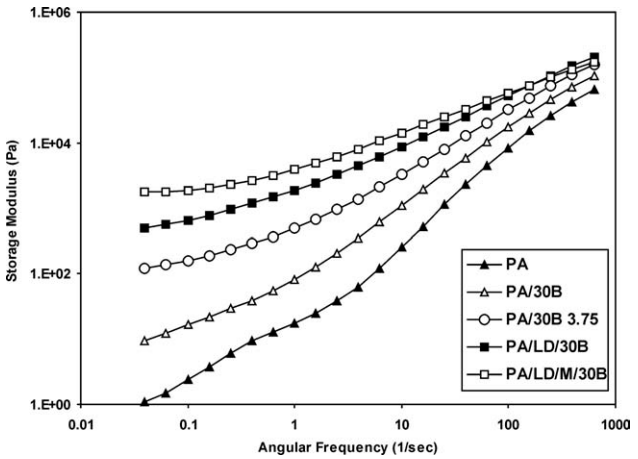

Figure 5 Rheological behavior of 3.75 wt % PA/Clay nanocomposite beside the rheological behavior of the other samples.

Clay exhibit liquid-like behavior in all frequency ranges, whereas the PA/Clay nanocomposite shows a pseudo solid-like behavior along the frequency. In other words, for PA/Clay nanocomposite tan δ increases with increasing of frequency at low frequencies (positive slope) and decreases after passing through a maximum (negative slope). Based on Winter-Chambon criterion,[29,30] this type of behavior is representative of the presence of solid-like network. In this case, the dispersion of clay platelets followed by their direct interaction and/or indirect interaction via chain bridging may be the main reason of appearance of solid-like behavior.[31]

The complex viscosity and storage modulus of PA/PE/Clay, PA/PE/PE-*g*-MA/Clay blend nanocomposites and their reference blends were plotted versus frequency in Figure 4. PA/PE blend shows liquid-like behavior similar to its components. When PE-*g*-MA was added to the blend, higher viscosity and storage modulus was achieved in high frequencies compared to PA/PE blend due to the formation of PA-*g*-PE copolymer, which has higher molecular weight than neat polymers. The generation of such a copolymer was evidenced using FTIR studies (section "FTIR analysis"). PA/PE/PE-*g*-MA ternary blend shows higher viscosity and storage modulus in low frequency region, indicating an enhanced interaction between two phases due to the formation of PA-*g*-PE interfacial agent and increased interfacial interaction in the melt state.

As the result show, adding of 3 wt % clay remarkably increased the storage modulus and complex viscosity of PA/PE blend and led to a more pronounced shear thinning and solid-like behavior at low frequencies. The ratio of storage modulus of different nanocomposites to reference samples at frequency of 0.0398 rad/s is presented in Table II.

TABLE II
Storage Modulus Ratio of Different Nanocomposites to Reference Samples

Storage modulus ratio of the nanocomposites ($\omega = 0.0398$ rad/s)		
Sample	Ref. Sample	G′ ratio
PA/30B	PA	8.43
LD/30B	LD	2.42
LD/M/30B	LD	6.81
PA/LD/30B	PA/LD	54.48
PA/LD/M/30B	PA/LD	191.04
PA/30B 3.75	PA	111.82

As the results show, the extent of increscent in elasticity of PA/PE blend with clay loading is much more than those of both neat PA and PE. Three probable mechanisms may involve in this increment:

1. Due to the higher affinity of clay to PA, which was concluded from rheological analysis, all the clay may locate in the PA phase leading to higher clay concentration in PA phase (3/80 = 3.75 wt % based on PA phase). This can increase the elasticity compared with 3 wt % PA/Clay nanocomposite. The rheological behavior of 3.75 wt % PA/Clay nanocomposite is presented in Figure 5 beside the rheological behavior of other samples and the extent of elasticity increment is taken in Table II for comparison. The results show that 3.75 wt % PA/Clay nanocomposite has higher but not too much higher elasticity compared with 3.0 wt % PA/Clay nanocomposite to justify that elasticity increment. So this mechanism cannot lonely be responsible for that increase and another mechanism should be involved.

2. It may be guessed that this increase is in the result of localization of clay at PA/PE blend interface and its compatibilizing effect. Due to the higher intercalation of clay in PA and low affinity of clay to PE, which is not also affected using the compatibilizer, the migration of clay toward the blend interface is low probable, and another mechanism should be considered.
3. The presence of elastic PE particles in intercalated PA/Clay matrix, can favor breaking down of intercalated clay tactoids leading to increased PA/Clay interface and increased probability of clay network formation. It should be noted that due to the lower molecular weight of PA, intercalation of clay with PA chains is an easy and fast process, but an effective stress is needed to exfoliation of such an intercalated clay tactoids. Lower viscosity of PA hinders the stress transfer to clay tactoids. In the presence of elastic PE particles, the stress can effectively transfer to tactoids. Moreover, when two PE particles move close to each other during the mixing process, the matrix between these particles drains away, providing deformation field, which can also be responsible for tactoids' break down. In this case, the XRD results should support the ideas.

From the obtained results and the discussion made above, it can be finally concluded that the main reason of increase in rheological behavior is the conjunction of mechanisms 1 and 3. In other words, higher clay content in PA phase and their detachment due to the PE particles' effect, leads to creation of higher PA/Clay interface and therefore a strong network formation. It is well known that interacting heterogeneous structures results in an apparent yield stress that is visible in dynamic measurements by a plateau of storage modulus at low frequencies.[32] The upturn of viscosity in conjunction with the nonterminal behavior of elasticity at low frequencies, observed for PA/PE/Clay and PA/PE/PE-*g*-MA/Clay nanocomposites are indicative of solid-like behavior corresponding to the creation of three-dimensional percolated tactoids' network with a strong adhesion to PA matrix. Such a network may result from either direct interaction between particles[33,34] or polymer-filler networking processes.[35,36]

The plateau region is larger (started at higher frequencies) for PA/PE/PE-*g*-MA/Clay blend nanocomposite than that of PA/PE/Clay due to better dispersion of the organoclay in the former sample. It is obvious that with addition of PE-*g*-MA, dependency of storage modulus on frequency decreases sharply at low frequency zone and it exhibits a distinct plateau. This indicates that addition of PE-*g*-MA can improve the compatibility between the polymer phase and the clay phase, resulting in the formation of much more clay tactoids than that of PA/PE/Clay sample. Therefore, the percolation network will evolve into the one with more perfect form and compact structure because of the enhancement of network density, leading to an increment in low frequency dynamic modulus of the ternary hybrids.

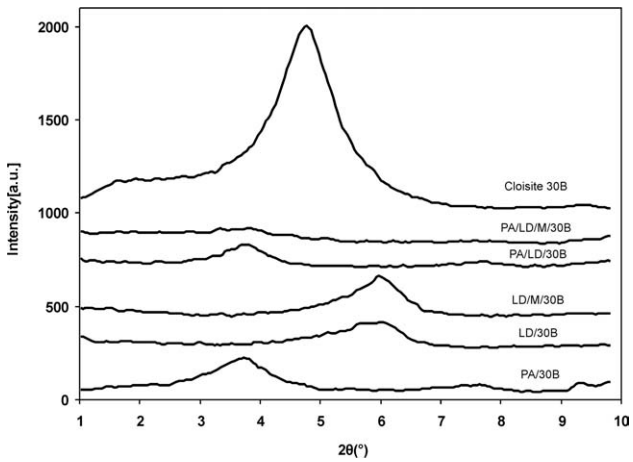

Figure 6 XRD patterns of Cloisite 30B, PA/Clay, PE/Clay, PE/PE-*g*-MA/Clay, PA/PE/Clay, and PA/PE/PE-*g*-MA/Clay.

It is worth to note that at high frequencies all the samples exhibit comparable values of storage modulus. This indicates that at these frequencies the response of the samples are weakly affected by the nanostructure and interfacial interaction and determined mainly by the matrix polymer.[37] Qi et al.[38] concluded that high frequency region corresponds to the segmental motion of polymer molecules.

The obtained results from the rheological studies clearly show that the melt linear viscoelastic behavior of the nanocomposites has a reliable sensitivity for evaluation of the extent of clay dispersion.

Morphology characterization

XRD results

XRD is based upon the interference pattern produced by repetitive structures in the organoclay and was used to investigate the microstructure and state of dispersion of the organoclay within the nanocomposites. XRD pattern of clay reflects the ordered arrangement of silicate layers. The penetration of polymer chains into clay interlayer (intercalation) results in an increase in d-spacing and a shift of XRD peaks to lower angles. A further shift to lower angles and a broadening or disappearing of the characteristic XRD peaks are indications of partial or complete exfoliation of the ordered clay structure.[31]

XRD patterns for the pure clay and its nanocomposites are presented in Figure 6. It should be noted that the characteristic XRD peaks of the PA and PE

TABLE III
Angular Location of the XRD Peaks and the Interlayer Spacing, d_{001} of Different Nanocomposites

Angular location and d-spacing of all the nanocomposites		
Sample	2θ (°)	d_{001} (nm)
Cloisite 30B	4.77	1.85
PA/30B	3.69	2.39
PA/30B 3.75	3.7	2.38
LD/30B	5.87	1.51
LD/M/30B	5.95	1.48
PA/LD/30B	3.73	2.36
PA/LD/M/30B	3.74	2.37
PA/(LD/M/30B)	3.81	2.31

crystals do not appear in this angular ranges. From the angular location of the peaks and the Bragg's equation [eq. (1)] the interlayer spacing (d_{001}) of the clay in each sample was determined and summarized in Table III.

$$2d \sin \theta = n\lambda, \quad (1)$$

where d is the distance between crystallographic planes, and θ is half of the angle of diffraction, n is an integer and λ is the wavelength of the X-ray.

The results show that the virgin clay exhibits a single diffraction peak at 2θ of 4.77°, which corresponds to a d-spacing of 1.85 nm. The diffraction peak of PA/Clay nanocomposite has shifted to lower angles and it displays lower intensity compared to pure clay, representative of an intercalated and/or a mixture of intercalated and exfoliated morphology. This can be attributed to the strong interaction between the PA chains and the platelets of organoclay. Cloisite 30B has two hydroxyl ethyl groups (—CH_2—CH_2OH) in its modifier. These groups could provide hydrogen bonding with PA and improve the compatibility.[39] Therefore, PA molecules can easily maintain contact with the surface of the organoclay layers. However, it can be concluded that the clay has not completely been exfoliated in PA matrix at this process condition and only a part of the PA chains has diffused into the interlayer of clay platelets. In PA nanocomposites, the adjacent layers may be bridged by the PA chains. Therefore, it is difficult to form the exfoliated structure only by the diffusion of PA molecules. In other words, the PA can glue the two surfaces together as it moves through the interlayer and thereby the chains of the PA cannot push the sheets to delaminate.[40] Moreover, the shear stress transferred by PA matrix cannot provide enough force to make organoclay exfoliated, judging from rheological properties and the torque of internal mixer which is not presented here. Therefore, it can be concluded that shear stress plays a crucial role in the exfoliation process of organoclay. The similar results for PA12 nanocomposites have been reported, that is, long mixing times and high blade rotational speeds lead to a good dispersion and a well-exfoliated structure.[41] Finally, considering the rheological and XRD results of this sample, it can be concluded that intercalated morphology has been achieved. However, as it can be seen in Figure 6, there is an additional peak at 2θ of 7.8° in XRD pattern of the PA/Clay sample. The appeared additional peak can be related to intercalation of unmodified fraction of nanoclay particles taking place during the melt mixing or the collapsing of modified clay layers in the result of degradation of clay modifiers at such elevated temperatures.[42]

Conversely, it can be seen that in PE/Clay nanocomposite, there is no indication that intercalation or exfoliation occur. Even a collapsed structure was achieved concluded from the shifting of the peak to higher angles. PE is not compatible with the modifier present in Cloisite 30B. In such a case, the collapsing could be due to the degradation of modifier and/or induced forces via PE matrix. It has been shown that the organoclay modifying ethyl ammonium group of Cloisite 30B degrades quite rapidly in the temperature range of 200–300°C.[21] Since the process conditions used to melt compounding fall in this range, the collapsed structure of the PE/Clay sample could be due to the thermo-degradation of the organomodifier and loss of surfactant mass from the clay galleries at high temperature melt processing. The results of Figure 6 indicate that the compatibility of the clay modifier with the polymer matrix is very important in the intercalation process.

It is worth noting that the intensity of XRD diffraction peak for PE/Clay sample has been reduced compared to PA/Clay diffraction peak. This shows that although PE molecules cannot diffuse into clay galleries contrary to PA chains, but due to the higher viscosity and therefore effective stress transfer, the clay tactoids can easily break down in PE matrix than that of PA matrix.

It was expected that addition of PE-*g*-MA improve the compatibility between the clay and PE matrix, leading to intercalation of the clay. Surprisingly, the XRD results showed that the presence of PE-*g*-MA compatibilizer does not only increase d-spacing but also decreases interlayer spacing of the clay and enhances the diffraction peak intensity compared to PE/Clay nanocomposite. One possible reason for the latter could be the obstructing effect on the chain diffusion by the excessive compatibilizer, which might congregate on the silicate surface and envelop the tactoids.[43] In other words, this could be due to physical jamming of the compatibilizer molecules around tactoids leading to hindering the break down of them. This would enhance the peak intensity. Moreover, in this sample thermodegradation of

clay modifier was occurred. The collapse of some fraction of the nanoparticles in the presence of compatibilizer was observed in a similar study.[28] These results confirm the obtained results from the rheological studies.

The intensity of the characteristic peak of the clay in PA/PE/Clay has sharply reduced and a broad peak can be observed at about $2\theta = 3.73$ ($d_{001} = 2.36$ nm). This suggests that the structure is at least intercalated. The XRD pattern of PA/PE/Clay nanocomposite indicates a high degree of the organoclay dispersion. Therefore, it can be concluded that the most of clay tactoids have been exfoliated. Comparing the XRD peaks of the samples PA/PE/Clay and PA/Clay indicates that the presence of PE clearly decreases the peak intensity while it slightly decreases the d-spacing of the clay. The former is in a good agreement with the obtained results using rheological studies and supports the idea of effective break down of the clay structure in the presence of PE particles. The latter can be due to the fact that PE, which can not diffuse in clay galleries, occupies the effective volume of the matrix and therefore the clay concentration is increased in PA phase, which in turn leads to limited intercalation. The exfoliation of organoclay in the PA matrix could be attributed to higher melt viscosity of the PE particles, which can provide stronger shear stress during melt mixing for delamination of the clay platelets.[44] This had been predicted using rheological studies and it confirms that the rheological properties have reliable sensitivity to the structure of the clay in polymer matrixes.

Considering the XRD pattern and rheological behavior of PA/PE/Clay sample indicates that in this nanocomposite the concentration of the organoclay falls above percolation level and some montmorillonite network is formed. Since dispersed PE particles has higher viscosity than that of PA phase, in the presence of PE higher stress may be applied on the clay tactoids and as a result many clay layers may detach from the big tactoids.

It is interesting to note that using PE-*g*-MA compatibilizer causes to more decrease in peak intensity and the diffraction peak has nearly been disappeared, while it does not have a clear effect on the d-spacing of the clay. This is in the result of more effective stress transfer in the presence of PE-*g*-MA. In the presence of PE-*g*-MA the PA-*g*-PE copolymer is formed (section "FTIR analysis") and located at the blend interface. It causes to better adhesion of PA and PE phases leading to formation of small but well adhered PE particles to PA matrix. Therefore, it can be concluded that although PE-*g*-MA cannot lonely intercalate the clay, but it forces the clay tactoids to aggregate around the PE particles. This can also reduce the intensity of the peak.[15,16]

SEM analysis

To investigate further, the effect of clay and compatibilizer on the morphology of polymer blends, SEM analysis was conducted on the PA/PE/Clay and PA/PE/PE-*g*-MA/Clay nanocomposites and their reference samples. Figure 7 shows SEM micrographs of different samples. In these images, the black void left by PE on PA phase is visible. The PA/PE blend exhibits brittle plastic deformation and a globular microstructure, with the PE minor phase forming spherical droplets suspended in PA matrix [Fig. 7(A)]. Due to the high interfacial tension and weak interfacial adhesion between the two immiscible polymers, the spherical morphology is the most thermodynamically favored as it leads to minimum of the specific interfacial area. The compatibilized blend using PE-*g*-MA [Fig. 7(B)] exhibits remarkably reduced dispersed particle size due to the effect of *in situ* formed copolymer at the interface.[21,39,45] The formation of such copolymer was evidenced using FTIR measurements (section "FTIR analysis").

SEM micrograph of PA/PE/Clay [Fig. 7(C)] shows that the presence of clay decreases the dispersed particle size. Decrease of dispersed particle size of the blends with clay incorporation has previously been reported in many studies.[21,39,46–48] There are different mechanisms to reduce the particle size:

1. If the clay locates at the interface of PA matrix and dispersed PE phase, it can play the role of an interfacial agent leading to reduce the interfacial tension and decreases the PE particle size.
2. If the clay is intercalated and/or exfoliated in PA matrix, it increases the matrix viscosity and capillary number and hence decreases viscosity ratio leading to increased droplet break up and therefore reduced PE particle size.
3. Localization of intercalated and in particular exfoliated clay platelets in blend matrix hinders particle coalescence and then decreases particle size.

In the case of PA/PE with PA as a matrix phase, localization of clay at the interface is less probable and it seems the decreased disperse/matrix viscosity ratio in conjunction with reduced particle coalescence are the most probable mechanisms in this case.

However, PE-*g*-MA is more effective than that of the clay in reducing of the particle size. Using PE-*g*-MA leads to formation of PA-*g*-PE copolymer, which is preferentially, locates at the interface while the clay almost localizes at the PA matrix and it cannot play the role of a proper compatibilizer in interfacial adhesion. The particle size decreases effectively if both clay and PE-*g*-MA are used simultaneously.

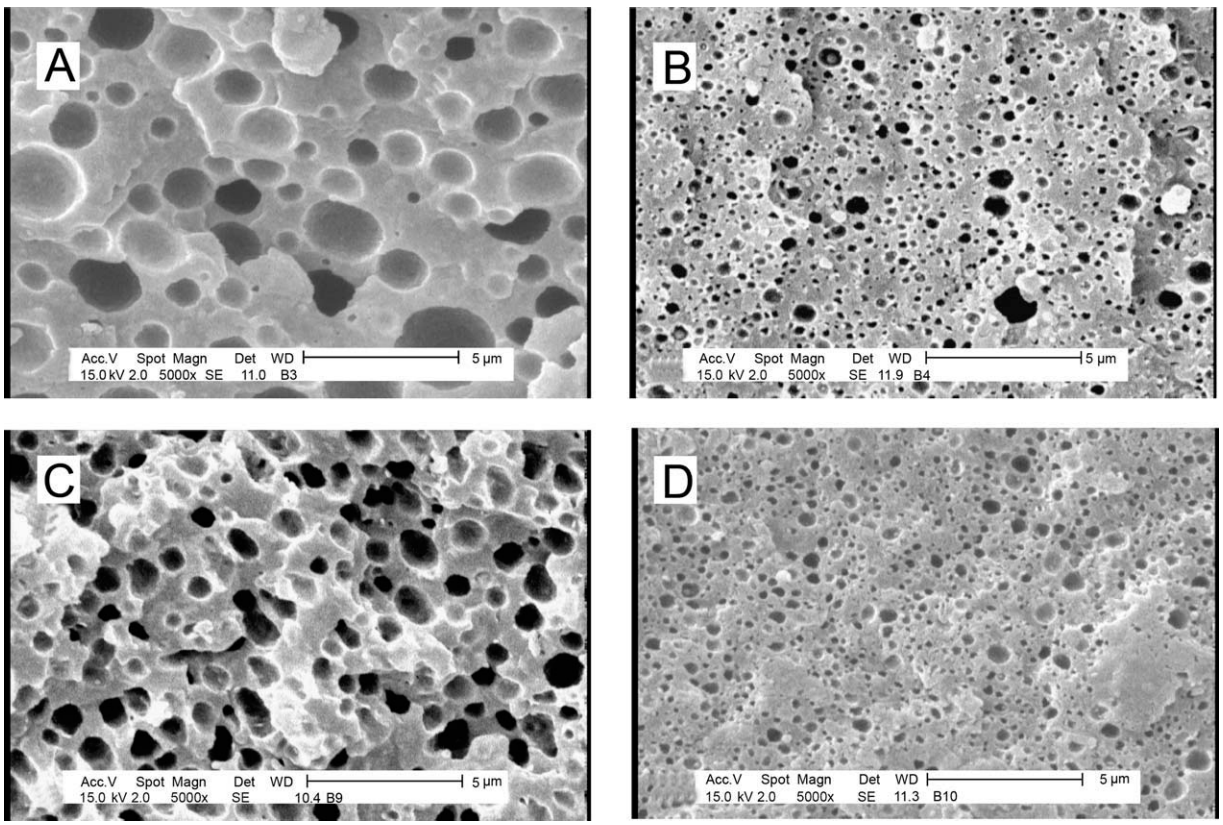

Figure 7 SEM micrographs of (A) PA/PE, (B) PA/PE/PE-*g*-MA, (C): PA/PE/Clay, and (D) PA/PE/PE-*g*-MA/Clay samples.

TEM analysis

Figure 8 shows TEM micrograph of PA/PE/PE-*g*-MA/Clay nanocomposite. The dark lines are the silicate layers. This image shows that the clay platelets are highly dispersed in PA matrix and confirms the obtained results from rheology and XRD studies. In addition, the presence of a significant numbers of exfoliated clay layers near the blend's interface could be due to the formation of PE-*g*-PA copolymer and its locating at the blend interface.

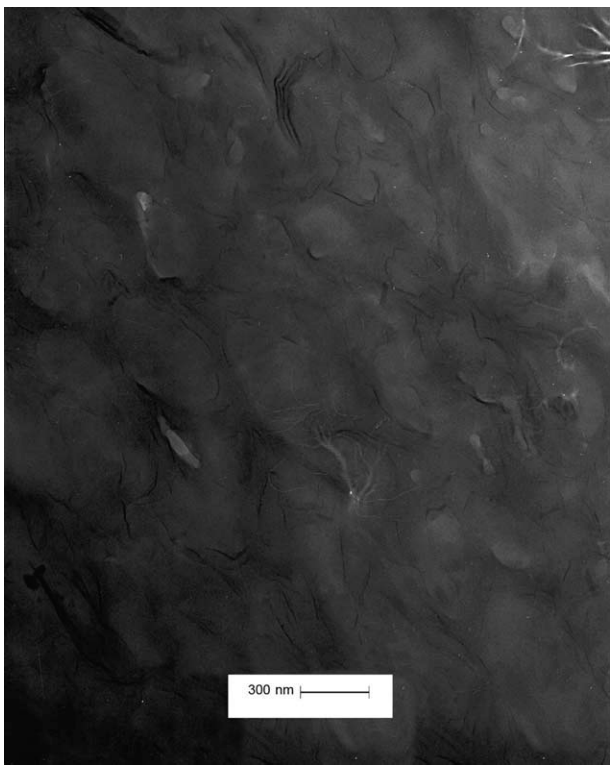

Figure 8 TEM micrograph of PA/PE/PE-*g*-MA/Clay sample.

EFFECT OF FEEDING ORDER

As the results of previous analyses showed, the clay locates at the PA matrix and does not migrate into the dispersed PE particles. However, in some applications it may be needed that the clay localizes in the dispersed particles. It is expected that feeding sequence could alter the partitioning of the clay between phases. Therefore, it was decided to study the effect of feeding order on the clay morphology and its partitioning. For this purpose, another PA/PE/PE-*g*-MA/Clay sample was prepared using a two-step method. At the first step, the masterbatch of PE/PE-*g*-MA/Clay was prepared under the same condition as described in experimental section. Then

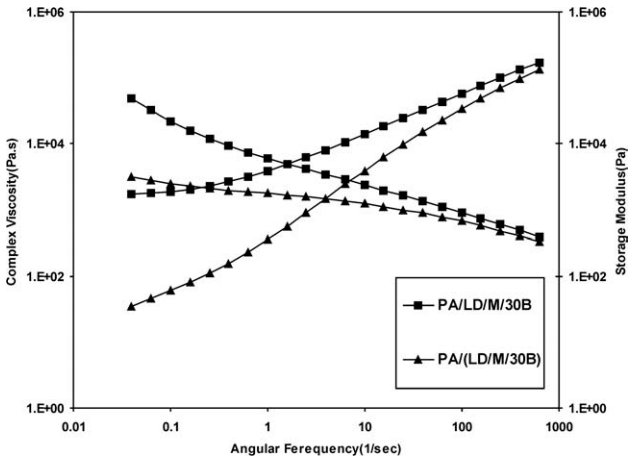

Figure 9 Storage modulus and complex viscosity versus angular frequency of PA/PE/PE-*g*-MA/Clay prepared using two different feeding orders.

the masterbatch was added to the melted PA to keep the compositions as same as the reference sample. This sample was named PA/ (PE/PE-*g*-MA/Clay).

Figure 9 shows the rheological properties of PA/(PE/PE-*g*-MA/Clay) and its reference sample. The results surprisingly show that the rheological properties of the samples prepared using different feeding orders are completely different. One-step prepared sample displays a pseudo solid-like behavior with a clear plateau at the terminal zone. As previously stated, this type of behavior is representative of the formation of a three dimensional network of the clay in PA matrix phase. The two-step prepared sample exhibits liquid-like behavior with lower elasticity. Based on the knowledge of the rheology of the nano\composites, the presence of the clay network in this sample is not probable and it may be suggested a not-intercalated morphology for clay in this sample. With reference to the fact that the clay can easily be intercalated in PA phase, this result implies that the clay could not migrate from PE dispersed phase to PA phase and the most probable morphology is dispersed PE/Clay composite droplets in PA matrix. A few part of the clay can leave the PE phase during shear mixing, but most of them are encapsulated by PE-*g*-MA in PE phase.

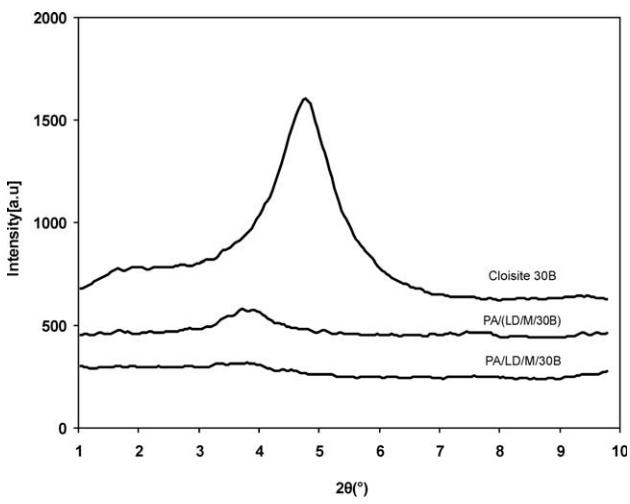

Figure 10 XRD patterns of Cloisite 30B and PA/PE/PE-*g*-MA/Clay prepared using two different feeding orders.

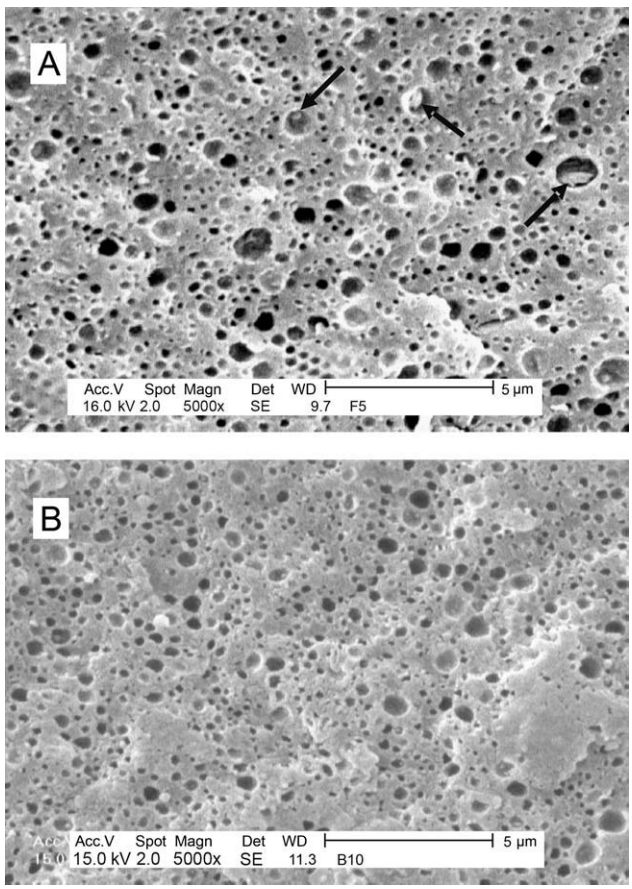

Figure 11 SEM micrographs of PA/PE/PE-*g*-MA/Clay prepared using (A) two-step and (B) one-step methods.

Figure 10 compares the XRD patterns of PA/PE/PE-*g*-MA/Clay nanocomposites prepared using different feeding orders as discussed earlier. Despite of their rheological behaviors, XRD patterns of the samples prepared using different feeding orders are near the same, corresponding to the intercalated morphology for both samples. From these results, it can be concluded that the morphology of the clay in the sample prepared via two-step method is intercalated. The results obtained in previous sections showed that PE chains can not diffuse into clay galleries to create an intercalated morphology. However, the results of rheological measurements implied that the clay could not migrate from dispersed PE particles to PA phase to form an intercalated morphology in PA phase. One possible mechanism for intercalation of clay in this sample can be presented as follows: Some part of PA diffuses to

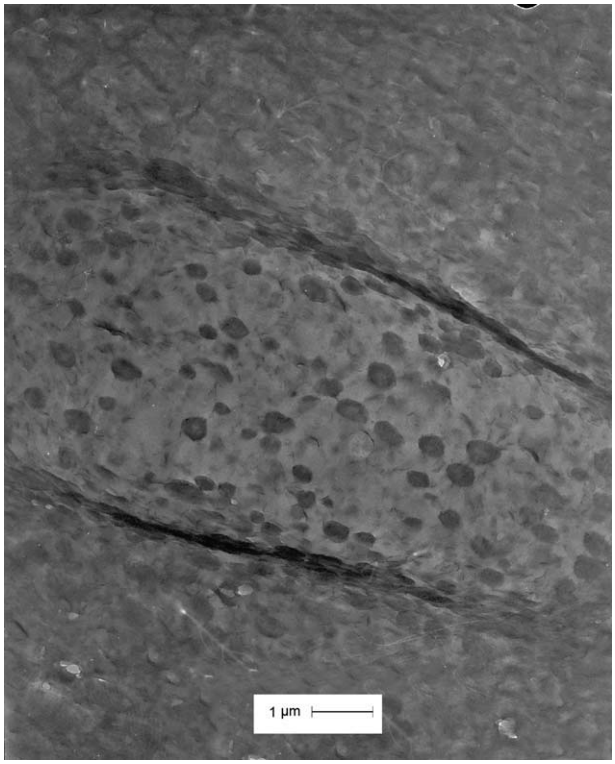

Figure 12 TEM micrograph of PA/(PE/PE-*g*-MA/Clay) sample prepared using two-step method.

PE/Clay composite droplets to intercalate the clay in that dispersed phase. Higher affinity of PA to clay and its capability to react with PE-*g*-MA may force the PA to diffuse to PE phase. If PA could diffuse to PE/Clay composite particles, the morphology would be expected to change from matrix/dispersed to phase within phase within phase morphology (PA in PE phase within PA continuous phase). In such a case, the size of composite droplets should be larger than that of one-step prepared reference sample. To confirm this claim, direct morphology observation should be applied. Figure 11 shows the SEM images of two samples prepared using different feeding orders. The results indicate the phase within phase within phase morphology for two-step prepared sample with bigger particle size. Trapped PA phase in some PE particles are shown with arrows. Higher intensity of the peak of two-step sample compared to one-step sample can be due to the higher clay concentration in PE phase ($\sim$ 15 wt %) and less applied stress to break down of the tactoids. Due to the low probability of clay intercalation in the two-step sample, the peak angular location has slightly shifted to higher angles. Based on Hedayati and Arefazar[16] encapsulation of the clay tactoids in the dispersed PE phase, even without intercalation, can also lead to reduce in peak intensity. Figure 12 shows the TEM image of the two-step prepared sample. The phase within phase within phase morphology can be seen in this image. These results clearly show that the rheological properties are more sensitive to clay localization than that of XRD patterns.

CONCLUSION

Relationship between the morphology and viscoelastic properties of PA/PE/Clay blend nanocomposites was studied. The rheological properties showed that an intercalated morphology could be achieved in PA/Clay nanocomposites while there was no affinity between clay and PE that was not improved using PE-*g*-MA compatibilizer. These results were confirmed by XRD studies. The rheological measurements also indicated that loading of clay onto PA/PE blend dramatically increases its viscosity and elasticity than that of pure PE and PA, especially in the presence of PE-*g*-MA compatibilizer. It was attributed to the detachment of intercalated clay layers in PA matrix phase due to the stress transfer from PE particles and deformation flow field created between PE particles, leading to formation of stronger network. It was shown that the nanocomposite with compatibilizer exhibited higher melt viscosity and storage modulus than the nanocomposite without compatibilizer, which was related to improved dispersion and polymer–silicate interactions for this sample. Considering the SEM results, it was concluded that in the presence of clay, more uniform and finer dispersion of minor phase was obtained due to enhanced matrix viscosity and reduced droplet coalescence. Feeding order was found to be an effective parameter on the clay dispersion and the morphology of the blends. When PE/PE-*g*-MA/Clay masterbatch was used to prepare PA/PE compatibilized nanocomposite, some part of PA phase migrated to PE phase and phase within phase within phase morphology was formed. While the results of XRD had not enough sensitivity for this type of the morphology, reliability of the results of rheological measurements were confirmed using TEM and SEM analyses.

References

1. Mittal, V. Eur Polym J 2007, 43, 3727.
2. Mittal, V. J Appl Polym Sci 2007, 107, 1350.
3. Maged, A.; Osman, A.; Mittal, V.; Ulrich, W. S. Macromol Chem Phys 2007, 208, 68.
4. Koha, H. C.; Parka, J. S.; Jeonga, M. A.; Hwanga, H. Y.; Hongc, Y. T.; Hab, Nam, S. Y. Desalination 2008, 233, 201.
5. Messersmith, P. B.; Giannelis, E. P. Chem Mater 1994, 6, 1719.
6. Vaia, R. A.; Sauer, B. B.; Tse, O. K.; Giannelis, E. P. J Polym Sci Part B: Polym Phys 1997, 35, 59.
7. Kyu, T.; Zhu, G. C.; Zhu, Z. L.; Tajuddin, Y.; Qutubuddin, S. J Polym Sci Part B: Polym Phys 1996, 34, 1769.
8. Tyan, H.; Liu, Y.; Wei, K. H. Polymer 1999, 40, 4877.
9. Yano, K.; Usuki, A.; Okada, A.; Kurauchi, T.; Kamigaito, O. J Polym Sci Part A: Polym Chem 1993, 31, 2493.

10. Kawasumi, M.; Hasegawa, N.; Kato, M.; Usuki, A.; Okada, A. Macromolecules 1997, 30, 6333.
11. Liu, L.; Qi, Z; Zhu, X. J Appl Polym Sci 1999, 71, 1133.
12. Incarnato, L.; Scarfato, P.; Scatteia, L.; Acierno, D. Polymer 2004, 45, 3487.
13. Weixia, Z.; Xiuying, Q.; Kang, S.; Guoding, Z.; Xiaodong, C. J Appl Polym Sci 2006, 99, 1523.
14. Wang, K.; Liang, S.; Du, R. N.; Zhang, Q.; Fu, Q. Polymer 2004, 45, 7953.
15. Hedayati, A.; Arefazar, A. Polym Compos 2009, 30, 1717–1731.
16. Hedayati, A.; Arefazar, A. Polym Test 2009, 28, 128.
17. Mehrabzadeh, M.; Kamal, M. R. Polym Eng Sci 2004, 44, 1152.
18. Klute, C. H.; Franklin, P. J. J Polym Sci 2003, 32, 161.
19. Lasoski, S. W.; Cobbs, W. H. J Polym Sci 2003, 36, 21.
20. Kamal, M. R.; Jinnah, I. A.; Utracki, L. A. Polym Eng Sci 2004, 24, 1337.
21. Filippone, G.; Dintcheva, N.Tz.; Acierno, D.; La Mantia, F. P. Polymer 2008, 49, 1312.
22. Okamoto, M.; Nam, P. H.; Maiti, P.; Kotaka, T.; Hasegawa, N.; Usuki, A. Nano Lett 2001, 1, 295.
23. Gagali, G.; Ramesh, C.; Lele, A. Macromolecules 2001, 34, 852.
24. Schmidt, G.; Nakatani, AI.; Butler, P. D.; Karimm A.; Han, C. C. Macromolecules 2000, 33, 7219.
25. Ren, J.; Silver, A. S.; Krishnamoorti, R. Macromolecules 2000, 33, 3739.
26. Krishnamoorti. R.; Yurekli, K.; Curr, O. Colloid Interface Sci 2001, 6, 464.
27. Pinnavaia, T. J.; Beall, G. W. Polymer-layered silicate nanocomposites; John Wiley & Sons: New York, 2001.
28. Pluta, M.; Jeszka, J. K.; Boiteux, G. Eur Polym J 2007, 43, 2819.
29. Chambon, F.; Winter, H. H. J Rheol 1987, 31, 683.
30. Winter, H. H.; Chambon, F. J Rheol 1986, 30, 367.
31. Rezanavaz, R.; Razavi Aghjeh, M. K.; Babaluo, A. A. Polym Comp 2010, 31, 1028.
32. Wang, K.; Liang, S.; deng, J.; Yang, H.; Zhang, Q.; Fu, Q.; Dong, X.; Wang, D.; Han, C. Polymer 2006, 47, 7144.
33. Mitchell, C. A.; Krishnamoorti, R. J Polym Sci Part B: Polym Phys 2002, 40, 1434.
34. Ren, J.; Krishnamoorti, R. Macromolecules 2003, 36, 4443.
35. Zhang, Q.; Archer, L. A. Langmuir 2002, 18, 10435.
36. Sarvestani, A. S.; Picu, C. R. Rheol Acta 2005, 45, 132.
37. Ren, J. X.; Shlva, A. S.; Krishnamoorti, R. Macromolecules 2000, 33, 3739.
38. Qi, L.; Dajun, C. Eur Polym J 2008, 44, 2046.
39. Mehrabzadeh, M.; Kamal, M. R. Can J Chem Eng 2002, 80, 1083.
40. Meng, X.; Wang, Z.; Zhao, Z.; Du, X.; Bi, W.; Tang, T. Polymer 2007, 48, 2508.
41. Mederic, P.; Razafinimaro, T.; Aubry, T. Polym Eng Sci 2006, 46, 986.
42. Nazockdast, E.; Nazockdast, H.; Goharpey, F. Polym Eng Sci 2008, 48, 1240.
43. Defeng, W.; Chixing, Z.; Xie, F.; Dalian, M.; Zhang, B. Polym Degrad Stab 2005, 87, 511.
44. Zhihao, Z.; Qiang, S.; Juan, P.; Jianbin, S.; Qingyong, C.; Junliang, Y.; Yumei, G.; Ronghua, J.; Xiaofeng, H.; Joong-Hee, L. Polymer 2006, 47, 8548.
45. Mederic, P.; Razafinimaro, T.; Aubry, T.; Moan, M.; Klopffer, M. Macromol Symp 2005, 75, 221.
46. Wu, D.; Zhou, C.; Zhang, M. J Appl Polym Sci 2006, 102, 3628.
47. Fang, Z.; Xu, Y.; Tong, L. Polym Eng Sci 2007, 47, 551.
48. Scaffaro, R.; Mistretta, M. C.; Mantia, F. P. Polym Degrad Stab 2008, 93, 1267.